BBA - Bioenergetics 1860 (2019) 148082

Contents lists available at ScienceDirect

BBA - Bioenergetics

journal homepage: www.elsevier.com/locate/bbabio

Does the water-oxidizing Mn_4CaO_5 cluster regulate the redox potential of the primary quinone electron acceptor Q_A in photosystem II? A study by Fourier transform infrared spectroelectrochemistry

Yuki Kato*, Ayaka Ohira, Ryo Nagao[1], Takumi Noguchi*

Division of Material Science, Graduate School of Science, Nagoya University, Furo-cho, Chikusa-ku, Nagoya 464-8602, Japan

ARTICLE INFO

Keywords:
Photosynthesis
Photosystem II
Plastoquinone
Redox potential
FTIR
Spectroelectrochemistry

ABSTRACT

Redox titration using fluorescence measurements of photosystem II (PSII) has long shown that impairment of the water-oxidizing Mn_4CaO_5 cluster upshifts the redox potential (E_m) of the primary quinone electron acceptor Q_A by more than 100 mV, which has been proposed as a photoprotection mechanism of PSII. However, the molecular mechanism of this long-distance interaction between the Mn_4CaO_5 cluster and Q_A in PSII remains unresolved. In this study, we reinvestigated the effect of depletion of the Mn_4CaO_5 cluster on $E_m(Q_A^-/Q_A)$ using Fourier transform infrared (FTIR) spectroelectrochemistry, which can directly monitor the redox state of Q_A at an intended potential. Light-induced FTIR difference measurements at a series of electrode potentials for intact and Mn-depleted PSII preparations from spinach and *Thermosynechococcus elongatus* showed that depletion of the Mn_4CaO_5 cluster hardly affected the $E_m(Q_A^-/Q_A)$ values. In contrast, fluorescence spectroelectrochemical measurement using the same PSII sample, electrochemical cell, and redox mediators reproduced a large upshift of apparent E_m upon Mn depletion, whereas a smaller shift was observed when weaker visible light was used for fluorescence excitation. Thus, the possibility was suggested that the measuring light for fluorescence disturbed the titration curve in Mn-depleted PSII, in contrast to no interference of infrared light with the PSII reactions in FTIR measurements. From these results, it was concluded that the Mn_4CaO_5 cluster does not directly regulate $E_m(Q_A^-/Q_A)$ to control the redox reactions on the electron acceptor side of PSII.

1. Introduction

In oxygenic photosynthesis, photosystem II (PSII) has a function as a light-driven water-quinone oxido-reductase, in which electrons are extracted from water and transferred to a plastoquinone molecule [1–4]. The thus obtained electrons are eventually used to reduce CO_2 to synthesize sugars. The photoreaction in PSII is initiated by charge separation between the special pair chlorophyll (Chl) P680 and the pheophytin electron acceptor $Pheo_{D1}$, forming a $P680^+Pheo_{D1}^-$ charged pair [5–7]. On the electron donor side, an electron hole on $P680^+$ is transferred to the redox-active tyrosine Y_Z and then to the Mn_4CaO_5 cluster, in which water oxidation is performed through a cycle of five intermediates (S_0–S_4) [8,9]. On the electron acceptor side, an electron is transferred from $Pheo_{D1}^-$ to the primary quinone electron acceptor Q_A and then to the secondary quinone electron acceptor Q_B (Fig. 1) [11,12]. These two plastoquinone molecules have significantly different functions; Q_A performs only a one-electron redox reaction and relays an electron from $Pheo_{D1}$ to Q_B, whereas Q_B can be doubly reduced to convert into plastoquinole by accepting two protons and then released into a thylakoid membrane.

It is known that PSII has various mechanisms of electron flow regulation for photoprotection by tuning the redox potentials (E_m's) of the cofactors mainly on the electron acceptor side. For instance, some cyanobacteria upshift the E_m of $Pheo_{D1}$ under strong illumination by changing its hydrogen bond interaction through the exchange of D1 protein isoforms [13,14]. Also, the E_m of single reduction of Q_B downshifts at a higher pH, accelerating relaxation of Q_B^- [15,16]. The most extensively examined redox reaction in the electron flow regulation of PSII is one-electron reduction of Q_A. This is because the redox state of Q_A reflects in the intensity of fluorescence from PSII, and hence it is readily monitored [17–20]. Using fluorescence detection, E_m of Q_A reduction ($E_m(Q_A^-/Q_A)$) has been estimated to be around −100 mV (vs. SHE) for oxygen-evolving PSII, and it has been shown that upon depletion of the Mn_4CaO_5 cluster, more specifically, upon removal of

* Corresponding authors.
E-mail addresses: yuki.kato@bio.phys.nagoya-u.ac.jp (Y. Kato), tnoguchi@bio.phys.nagoya-u.ac.jp (T. Noguchi).
[1] Present Address: Research Institute for Interdisciplinary Science, and Graduate School of Natural Science and Technology, Okayama University, Japan.

https://doi.org/10.1016/j.bbabio.2019.148082
Received 22 March 2019; Received in revised form 31 August 2019; Accepted 8 September 2019
Available online 25 October 2019
0005-2728/

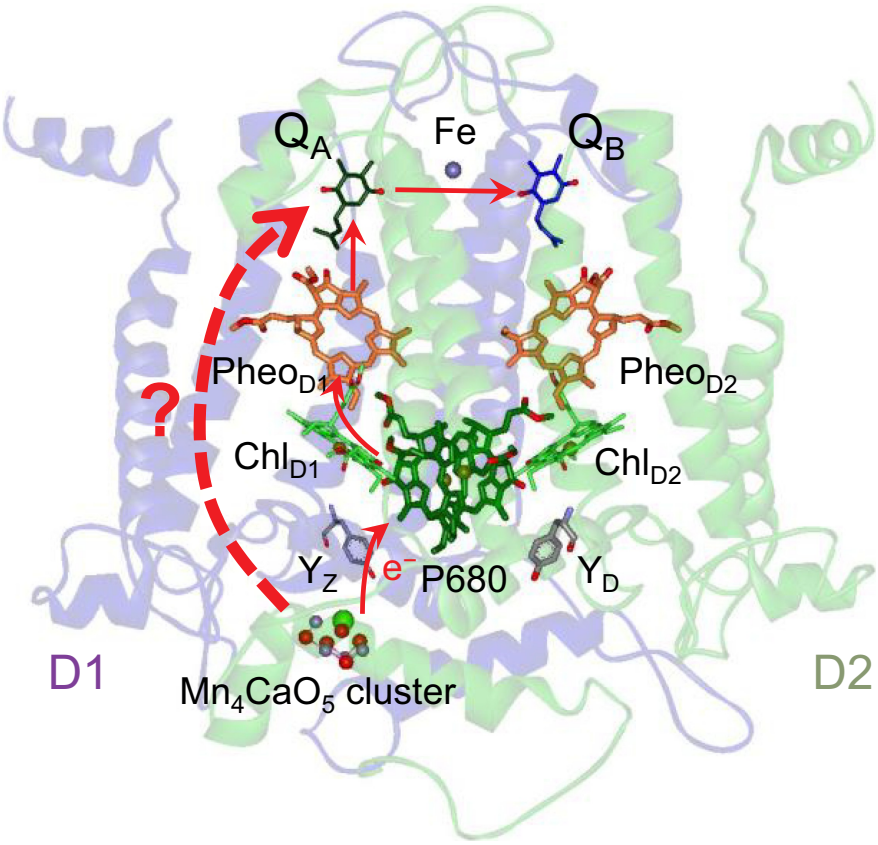

Fig. 1. Redox cofactors and the electron transfer pathway (red solid arrows) in PSII. A red dashed arrow indicates a putative, but yet to be identified, long-distance interaction between the Mn_4CaO_5 cluster and Q_A. The X-ray crystallographic structure at 1.9 Å resolution (PDB ID code: 3ARC) [10] was used for the PSII structure.

Ca^{2+} from it, $E_m(Q_A^-/Q_A)$ largely upshifts by 100–160 mV [21–29]. The physiological role of this $E_m(Q_A^-/Q_A)$ shift in photoprotection has been argued that the positive E_m shift promotes direct relaxation of Q_A^- to prevent the formation of harmful singlet oxygen through the triplet state of chlorophyll [7,30–32]. In addition, $E_m(Q_A^-/Q_A)$ has been shown to change by herbicide that binds at the Q_B site; PSII with 3-(3,4-dichlorophenyl)-1,1-dimethylurea (DCMU) has a higher $E_m(Q_A^-/Q_A)$ by ~100 mV than that with bromoxynil [23]. Furthermore, it was recently found that depletion of bicarbonate from the non-heme iron upshifts the $E_m(Q_A^-/Q_A)$ by ~75 mV, which was proposed to be a regulation mechanism in response to a CO_2 level [29].

Although the $E_m(Q_A^-/Q_A)$ regulation by herbicide and bicarbonate binding at the Q_B site and the non-heme iron, respectively, is reasonably understood by close interactions of Q_A with the non-heme iron and Q_B through the Q_A-His-Fe-His-Q_B bridge, the mechanism of the interaction between Q_A and the Mn_4CaO_5 cluster is hardly understood because they are separated at a long distance of ~40 Å. In addition, the Mn_4CaO_5 cluster is ligated mainly by amino acid ligands on the D1 subunit, whereas Q_A interacts with the D2 subunit. Because, no large E_m change was observed in Q_B and the non-heme iron by removal of the Mn_4CaO_5 cluster [33,34], the effect of Mn/Ca depletion on the Q_A site through the transmembrane helices of the D1 subunit and then the Q_A-His-Fe-His-Q_B bridge cannot be expected. Furthermore, our Fourier transform infrared (FTIR) study could not detect any appreciable changes in the Q_A interactions and nearby protein structures upon Mn depletion [35]. Also, it has been reported that there is no effect of Mn/Ca depletion on the redox equilibrium between Q_A^- and Q_B^- [15] and on the electron transfer rate from Q_A^- to Q_B [36] (but see ref. [37] reporting the effect of Ca^{2+} depletion on the decay kinetics of Q_A^-). Thus, the effects of Mn/Ca depletion on the Q_A reaction, which should reflect the $E_m(Q_A^-/Q_A)$ change, are still controversial, and the molecular mechanism of the long-distance interaction between the Mn_4CaO_5 cluster and Q_A remains unresolved.

In this study, we reinvestigated the effect of depletion of the Mn_4CaO_5 cluster on $E_m(Q_A^-/Q_A)$ using FTIR spectroelectrochemistry, which can directly monitor the redox state of Q_A by detecting Q_A-specific signals in contrast to indirect monitoring of the Q_A^- state by fluorescence detection. We already successfully used the FTIR spectroelectrochemical method [38] in combination with a light-induced difference technique [39–42] for the first direct measurement of the E_m of Q_B reduction using Q_B-specific signals [33]. The most significant advantage of FTIR spectroelectrochemistry is that infrared light to monitor the redox states of Q_A and Q_B does not interfere with the photoreactions in PSII, whereas fluorescence measurement requires visible light for fluorescence excitation that could influence the redox states of the cofactors even when using very weak light. Determination of the precise value of $E_m(Q_A^-/Q_A)$ is also of significance as an 'anchor point' in estimating the E_m values of other redox cofactors in PSII, which are too high to directly measure, such as P680 and Y_Z [43,44]. The FTIR data obtained using two different PSII preparations from spinach and a cyanobacterium *Thermosynechococcus elongatus* showed a surprising result that $E_m(Q_A^-/Q_A)$ was hardly affected by depletion of the Mn_4CaO_5 cluster. This result requires the essential change in the generally accepted view that the Mn_4CaO_5 cluster regulates the electron transfer reaction of Q_A by a long-distance interaction in PSII.

2. Materials and methods

2.1. Sample

Oxygen-evolving PSII membranes from spinach [45] were prepared as reported previously [46]. For Mn depletion, the PSII membrane sample in a pH 6.5 buffer containing 40 mM Mes, 5 mM, NaCl, 5 mM $CaCl_2$, 5 mM $NaHCO_3$, and 1 M glycine-betaine (Buffer A) was treated with 10 mM NH_2OH in the presence of 0.5 mM EDTA for 30 min on ice, followed by washing with Buffer A by centrifugation. PSII core complexes from the *T. elongatus* 47-H strain [47] were purified as described

previously [48]. For Mn depletion, the PSII core sample in a pH 6.5 buffer containing 40 mM Mes-NaOH, 5 mM NaCl, 5 mM $CaCl_2$, 0.06% DM (Buffer B) was treated with 10 mM NH_2OH in the presence of 0.5 mM EDTA for 30 min at room temperature, followed by washing with Buffer B with 10% (*w/v*) polyethylene glycol 6000 (PEG6000) by centrifugation. The O_2 evolution activities of the PSII preparations were measured using a Clark-type oxygen electrode at 25 °C under a saturating light condition. The O_2 evolution rate of the PSII membranes from spinach was ~500 μmol O_2 (mg Chl)$^{-1}$ h^{-1} in the presence of phenyl-*p*-benzoquinone (P*p*BQ) as an exogenous electron acceptor, while that of the PSII core complexes from *T. elongatus* was ~2480 μmol O_2 (mg Chl)$^{-1}$ h^{-1} in the presence of 2,6-dichloro-1,4-benzoquinone (2, 6-DCBQ). Upon Mn depletion, O_2 evolution was virtually lost in both the PSII preparations. SDS-PAGE analysis was performed as described previously [49].

2.2. FTIR spectroelectrochemical measurement

FTIR spectroelectrochemical measurement was performed as described previously [33,34,38]. The PSII membranes from spinach suspended in Buffer A additionally containing 0.1 mM DCMU, 200 mM KCl, and redox mediators [500 μM anthraquinone-2-sulfonate (E_m = −195 mV), 500 μM 2-hydroxy-1,4-naphthoquinone (E_m = −100 mV), 200 μM 1-methoxy-5-methylphanazinium methosulfate (methoxy-PMS; E_m = +63 mV), 200 μM *N,N,N′,N′*-tetramethyl-*p*-phenylenediamine (TMPD; E_m = +260 mV), and 4 mM potassium ferricyanide (E_m = +430 mV)] were centrifuged at 170,000 ×*g* for 35 min, and the resultant pellet was loaded onto an optically transparent thin-layer electrode (OTTLE) cell. For the PSII core complexes from *T. elongatus*, the PSII sample (0.2 mg Chl) suspended in Buffer B additionally containing 5 mM $NaHCO_3$, 1 M glycine-betaine, 10% PEG6000, 200 mM KCl, and the above redox mediators was centrifuged at 170,000 ×*g* for 15 min, the resultant pellet was loaded onto a OTTLE cell.

The OTTLE cell consisted of a gold mesh (60% transparent, 6 μm thickness; Precision Eforming LLC) working electrode, which was chemically modified with 4,4′-dithiodipyridine, a Pt black counter electrode, and a Ag/AgCl/3 M KCl reference electrode (Cypress Systems Inc., 66-EE009). The sample temperature was adjusted to 10 °C by circulating cold water in a holder of the OTTLE cell. The electrode potential of the OTTLE cell, referred against the standard hydrogen electrode (SHE), was controlled using a potentiostat (Toho Technical Research, Model 2000).

Light-induced FTIR difference spectra were recorded using a Bruker IFS-66/S spectrophotometer equipped with an MCT detector (D313-L/3) at 4 cm^{-1} resolution [33,34]. For the spinach PSII membranes, the sample in the presence of DCMU was equilibrated at an intended electrode potential for 60 min, and spectra with 20-s scans were recorded before and during illumination of continuous red light (12 mW/cm^2) from a halogen lamp (Hoya-Schott HL150) with a red filter (R60). Note that this red light is triggering light, which should be strong enough to saturate the photoreaction (reduction of neutral Q_A equilibrated at an intended electrode potential), whereas the measuring light is infrared light, which does not affect the photoreaction of PSII [38]. The period of 60 min for equilibration at an intended potential was adopted from the previous fluorescence spectroelectrochemical measurements of the redox potential of Q_A [24,25]. The sample was then incubated at +350 mV for 60 min to relax Q_A^-. A light-induced FTIR difference spectrum was measured to confirm the full oxidation of Q_A, and after further 30 min incubation at +350 mV, the sample was subjected to another intended potential. This measurement scheme (Fig. S1A in Supplementary material) was repeated to obtain FTIR difference spectra at a series of electrode potentials. A standard $S_2Q_A^-/S_1Q_A$ (intact PSII) or Q_A^-/Q_A (Mn-depleted PSII) difference spectrum was obtained as an average spectrum at +350 mV.

For the PSII core complexes from *T. elongatus*, a flash from a Q-switched Nd:YAG laser (Quanta-Ray INDI-40-10; 532 nm, ~7 ns full width at half maximum, ~7 mJ pulse^{-1} cm^{-2}) was used as triggering light. After incubation at an intended electrode potential for 60 min, one spectrum with 10-s scans was recorded before applying a single flash, and then five spectra with 2-s scans and subsequent five spectra with 10-s scans were recorded after the flash. The sample was then incubated at +350 mV for 60 min, and spectra (2-s scans) were measured before and after a single flash. After further 30 min incubation at +350 mV, the sample was subjected to another intended potential. This scheme (Fig. S1B) was repeated to obtain flash-induced FTIR difference spectra, representing the formation and subsequent relaxation of Q_A^-, at a series of electrode potentials, and a standard $S_2Q_A^-/S_1Q_A$ (intact PSII) or Q_A^-/Q_A (Mn-depleted PSII) difference spectrum as an average spectrum at +350 mV. An $S_2Q_B^-/S_1Q_B$ difference spectrum was measured using the intact PSII core sample identical to that described above except for the absence of the two quinone mediators, anthraquinone-2-sulfonate and 2-hydroxy-1,4-naphthoquinone [33]. Spectra with 10-s scans were recorded before and after a single flash at +350 mV, and the measurement was repeated four times with a dark interval of 30 min to obtain an average $S_2Q_B^-/S_1Q_B$ difference spectrum.

2.3. Fluorescence spectroelectrochemical measurement

Fluorescence spectroelectrochemical measurement was carried out following the previous method [24] with slight modification. The same OTTLE cell as in the FTIR spectroelectrochemical measurement was used for fluorescence measurement. Only the thickness of a gold mesh was changed to 140 μm in the case of a solution sample. Fluorescence measurements were performed for solution and pellet samples. The solution sample was the PSII core complexes from *T. elongatus* in the electrolyte solution identical to that used in the FTIR measurements (0.13 mgChl/mL; absorbance of the Qy band at ~673 nm was less than 0.18). The pellet sample was the same PSII core preparation in the presence of PEG as in the FTIR measurement but with a smaller amount (0.05 mg Chl; absorbance of the Q_y band was less than 0.3). The sample was incubated at each electrode potential for 60 min, and then a fluorescence spectrum was recorded using a JASCO FP6500 spectrofluorometer with weak monochromatic light (430 nm; 0.01 μE s^{-1} m^{-2} at the sample surface) for 60 s. For fluorescence measurement with weaker excitation light, the monochromatic light (430 nm) was attenuated by a factor of 10 using a neutral density filter (ND10).

3. Results

We adopted a combined methodology of FTIR spectroelectrochemistry and light-induced FTIR difference spectroscopy [38] for accurate estimation of the redox potential of Q_A. Because we detect very small infrared absorption changes (in the order of 10^{-4} as ΔA), two spectra before and after a reaction need to be measured with a relatively short interval to avoid baseline distortion. Higher-quality difference spectra can be obtained in light-induced FTIR difference measurement than electrochemically-induced FTIR difference measurement, which requires a long interval (~60 min, see Fig. S1) for redox equilibrium of Q_A. By applying saturating triggering light (continuous red light and a 532-nm flash for spinach and *T. elongatus* PSII samples, respectively), neutral Q_A is fully photoreduced to Q_A^-, and a light-induced FTIR difference spectrum is obtained using measuring infrared light, revealing the population of neutral Q_A before illumination in equilibrium at an intended electrode potential. FTIR difference spectra of the intact and Mn-depleted PSII membranes from spinach in the presence of DCMU were measured as under-minus-before continuous illumination at various electrode potentials between +250 and −200 mV (Fig. 2Aa, b). At the high enough potential of +250 mV, Q_A is fully oxidized before illumination, and upon photoreduction, the typical signals of Q_A^- formation were observed at 1478 and 1719 cm^{-1}, which have been assigned to the CO stretching vibration of

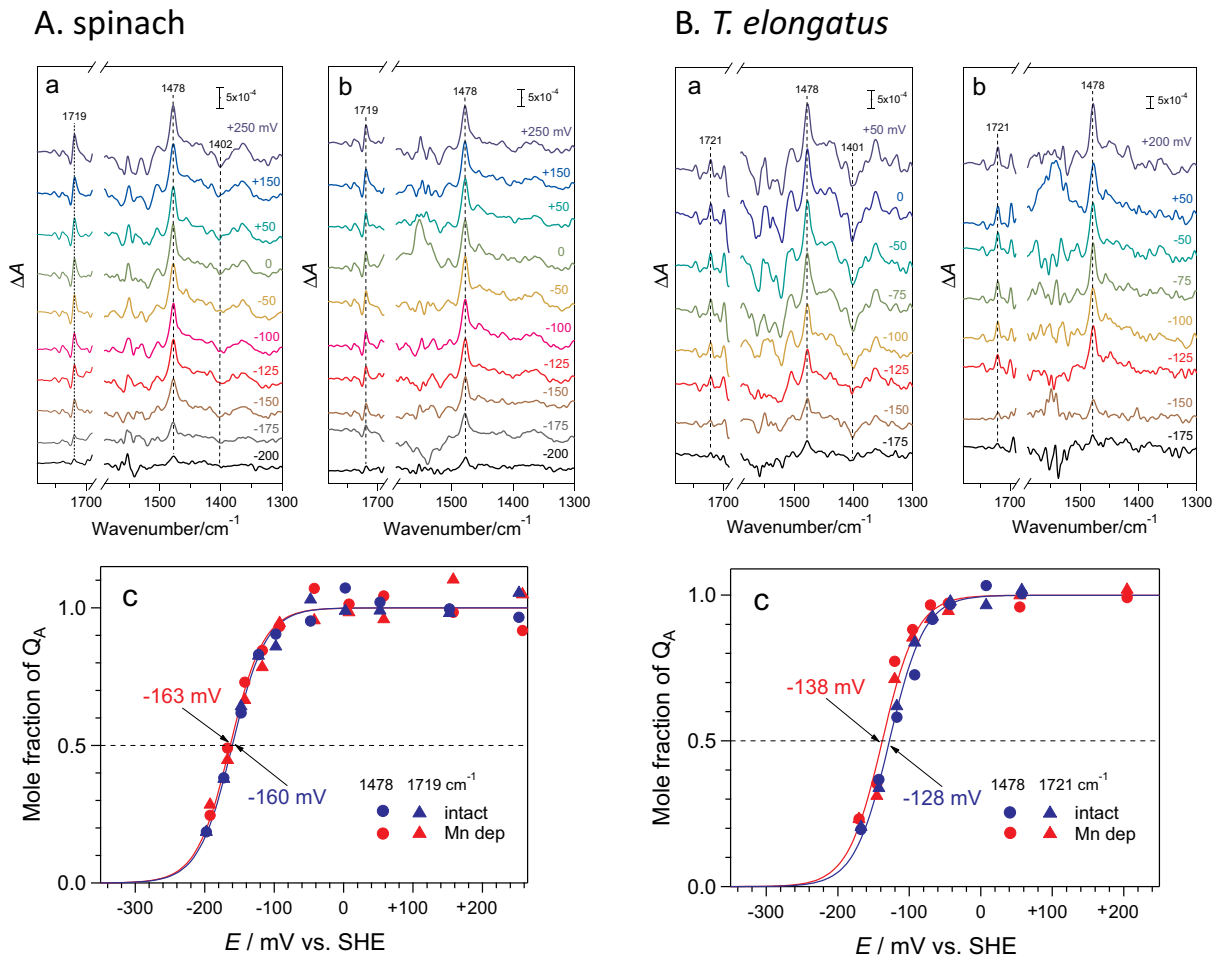

Fig. 2. Light-induced FTIR difference spectra of the (a) intact and (b) Mn-depleted PSII preparations at a series of electrode potentials and (c) the Nernst plots of the redox reactions of Q_A. (A) PSII membranes from spinach; (B) PSII core complexes from *T. elongatus*. For the PSII membranes from spinach, continuous light was illuminated to the sample in the presence of DCMU and difference spectra of during minus before illumination were obtained, while for the PSII core complexes from *T. elongatus*, a single flash was applied to the sample in the absence of herbicide and difference spectra of after minus before illumination were obtained. The 1700–1600 cm^{-1} region is saturated by strong absorption due to the amide I and water bending vibrations. In (c), the relative intensities of the peaks at 1478 (circles) and at 1719–1721 (triangles) cm^{-1} were plotted for the intact (blue symbols) and Mn-depleted (red symbols) PSII preparations. One-electron Nernst curves obtained by fitting the data involving both the 1478 and 1719–1721 cm^{-1} intensities are superimposed in the same color with estimated E_m values as mid-point potentials.

a Q_A^- semiquinone anion and the ester CO vibration of $Pheo_{D1}$ near Q_A, respectively [50–52]. In the intact PSII membranes, an additional signal was observed at 1402 cm^{-1} as a typical band of an S_2/S_1 difference spectrum arising from the symmetric COO^- stretching vibrations of carboxylate groups around the Mn_4CaO_5 cluster [53–55] (Fig. 2Aa), ensuring the intactness of the Mn_4CaO_5 cluster. In contrast, in the Mn-depleted PSII membranes, the 1402 cm^{-1} band was not observed (Fig. 2Ab), which was more clearly seen in a standard Q_A^-/Q_A spectrum obtained at +350 mV (Fig. S2Aa). When the electrode potential was lowered, the intensities of the bands at 1478 and 1719 cm^{-1} little changed up to −100 mV and then gradually decreased until they became very weak at −200 mV. These decreases in the photo-induced signals are due to prereduction of Q_A and hence reflect the population of Q_A^- equilibrated at a poised electrode potential before illumination. Note that the stabilities of the PSII samples during a series of measurements were verified by the amplitudes of the $S_2Q_A^-/S_1Q_A$ or Q_A^-/Q_A difference spectra measured at +350 mV every time before the measurements at intended potentials (Fig. S3A). The Nernst plots of Q_A reduction were drawn from the intensities of the 1478 and 1719 cm^{-1} bands in the FTIR difference spectra (Fig. 2Ac). Fitting of the plots using a one-electron Nernst equation showed very similar $E_m(Q_A^-/Q_A)$ values of −160 ± 2 and −163 ± 2 mV for the intact and Mn-depleted PSII membranes, respectively (Table 1). Although either of these E_m values was obtained by the measurements using one sample, reproducibility of the E_m value obtained by the present FTIR method was confirmed by the measurements of two other samples of intact PSII membranes from spinach. The Nernst plots of the data by these measurements provided the E_m values of −158 ± 2 and −162 ± 2 mV, which agree well

Table 1
Redox potentials (mV) of Q_A in intact and Mn-depleted PSII estimated by FTIR and fluorescence spectroelectrochemical measurements.

Sample	Method	E_m (mV)[d]		
		Intact	Mn-depleted	ΔE_m (mV)[b]
Spinach PSII membranes[a]	FTIR	−160 ± 2	−163 ± 2	−3 ± 3
T. elongatus PSII core complexes	FTIR	−128 ± 2	−138 ± 3	−10 ± 4
	Fluorescence	−110 ± 5	+6 ± 3 (−32 ± 3)[c]	+116 ± 6

[a] PSII membranes in the presence of DCMU.
[b] E_m change upon Mn depletion.
[c] Measuring light (430 nm) was attenuated by a factor of 10 using a neutral density filter.
[d] Error in the E_m value is the standard deviation of E_m as a parameter in the least-squares fitting of the Nernstian plot.

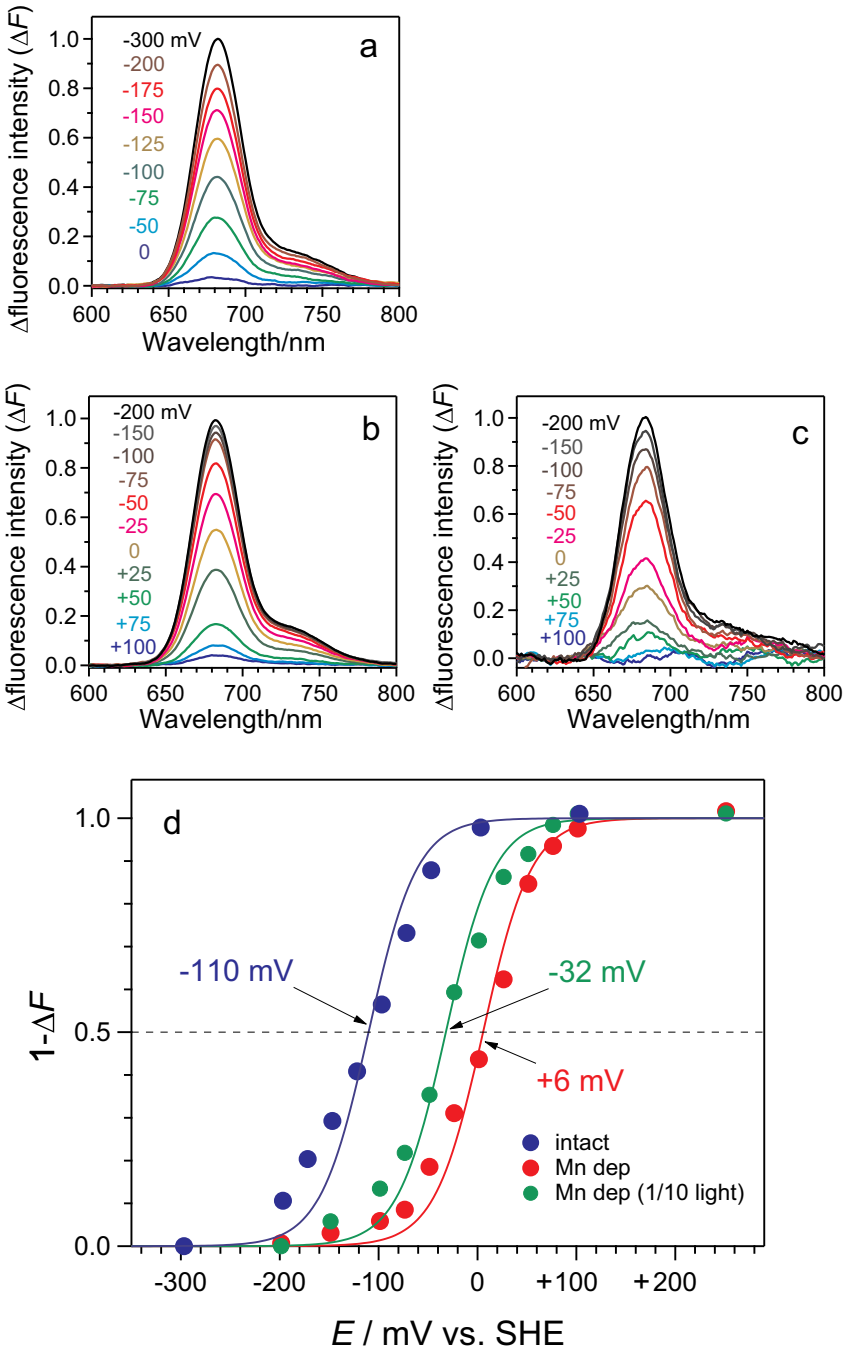

Fig. 3. (a–c) Electrochemically reduced-minus-oxidized fluorescence difference spectra of the (a) intact and (b, c) Mn-depleted PSII core complexes from *T. elongatus* at a series of electrode potentials. A fluorescence spectrum, which was measured at +100 mV and +250 mV for the intact and Mn-depleted PSII complexes, respectively, was subtracted from spectra measured at other electrode potentials. Spectra in (c) were measured with excitation light (430 nm) attenuated by a factor of 10. (d) Nernst plot of $1 - \Delta F$ (ΔF: intensity of the fluorescence difference) for the intact (blue circles) and Mn-depleted (red and green circles) PSII. Data of Mn-depleted PSII measured using ten times weaker light are shown in green circles. One-electron Nernst curves obtained by fitting the data are superimposed in the same color with estimated E_m values as mid-point potentials.

enough with the above value of -160 ± 2 mV. The Nernst plot of the relative intensities of the S_2/S_1 band at 1402 cm^{-1} in the spectra of the intact PSII membranes also showed a curve close enough to that of the Q_A^-/Q_A signal (Fig. S4A), confirming that the $S_1 \rightarrow S_2$ transition upon illumination was coupled with the reduction of Q_A.

The redox equilibrium of Q_A at different electrode potentials was further examined using the PSII core complexes from a cyanobacterium *T. elongatus*. A single flash from a Nd:YAG laser as triggering light was applied to the sample in the absence of herbicide to detect the photoreduction of Q_A using FTIR difference spectroscopy. The reason for the avoidance of herbicide in this measurement is that reoxidation of Q_A^- was significantly slow in the *T. elongatus* core complexes with herbicide. Flash-induced FTIR difference spectra of the intact and Mn-depleted PSII core complexes were measured at a series of electrode potentials (Fig. 2Ba, b). Again, typical peaks of the Q_A^-/Q_A difference spectrum due to the CO stretch of Q_A^- and the ester CO stretch of $Pheo_{D1}$ were observed at 1478 and 1721 cm^{-1}, respectively, at high electrode potentials. The intact core complexes also showed a COO^- band of the S_2/S_1 difference at 1401 cm^{-1} (Fig. 2Ba), whereas this band was absent in the Mn-depleted core complexes (Figs. 2Bb and S2Ba). It is noted that even at a very high potential of +350 mV, Q_B^-/Q_B signals with a typical peak at 1745 cm^{-1} arising from the ester C=O vibration of $Pheo_{D2}$ [51] were not observed (Fig. S2Bb), in contrast to our previous FTIR spectroelectrochemical measurements of Q_B [33]. In the present measurements, two quinone mediators, anthraquinone-2-sulfonate and 2-hydroxy-1,4-naphthoquinone, which were not used in the previous Q_B measurements, were included in the redox mediators. When these mediators were removed, the Q_B^-/Q_B signals with a peak at 1745 cm^{-1} were observed at +350 mV (Fig. S2Bc). It is thus suggested that either of these quinone mediators occupied the Q_B pocket at least at higher

electrode potentials and blocked the electron transfer from Q_A^- to Q_B. At lower electrode potentials, Q_B is doubly reduced (E_m values of the single and double reduction of Q_B were previously estimated to be ~ +90 and ~ +150–220 mV, respectively, in the intact and Mn-depleted PSII core complexes from *T. elongatus* [33]) and the quinone mediators are also mostly reduced, and hence the Q_B pocket is most likely empty.

When the electrode potential was lowered, the intensities of the 1478 and 1721 cm^{-1} bands in the intact and Mn-depleted PSII core complexes were virtually unchanged up to −75 mV and then gradually decreased. At −175 mV, the intensities were very weak in both samples. Again, the stabilities of the PSII core complexes throughout the experiment were verified by flash-induced measurements at +350 mV performed before the measurements at individual electrode potentials (Fig. S3B). The flash-induced Q_A^- signal decayed in two phases with a relatively fast (τ ~ 10 s) and very slow (τ > minutes) rates, and the relative amplitude of the fast phase increased at higher electrode potentials (Fig. S5). The fast phase may originate from reoxidation of Q_A^- by the quinone mediator occupied in the Q_B site, whereas the very slow phase may be attributed to Q_A^- reoxidation in centers with the empty Q_B site by free redox mediators in solution. In the case of the intact PSII core complexes, charge recombination of Q_A^- with the S_2 state on the electron-donor side may also contribute to the fast decay phase in competition with rereduction of the S_2 state by redox mediators. Due to the presence of the fast phase, the Q_A^- signal slightly decays even during the first measurement (2-s scan) after a flash at higher electrode potentials. Thus, to accurately estimate the amount of the photoreduced Q_A, the intercepts of the fitting curves were taken as the real intensities of the Q_A^-/Q_A signals (Fig. S5). One-electron Nernst curves fitting the mole fractions of Q_A estimated from these intensities (Fig. 2Bc) showed that the $E_m(Q_A^-/Q_A)$ values of the intact and Mn-depleted PSII core complexes from *T. elongatus* were −128 ± 2 and −138 ± 3 mV, respectively (Table 1), which were again very similar with only a small difference of −10 ± 4 mV. Note that the Nernst plot of the S_2/S_1 signal at 1401 cm^{-1} in the intact PSII core complexes virtually followed that of the Q_A^-/Q_A signal (Fig. S4B).

The estimated $E_m(Q_A^-/Q_A)$ value of the intact PSII preparation from *T. elongatus* (−128 mV) was slightly higher than that of the PSII preparation from spinach (−160 mV). This difference in $E_m(Q_A^-/Q_A)$ between *T. elongatus* and spinach may be attributed to species dependence, because the same trend was previously observed in the intact PSII preparations from these species [24,25]; the $E_m(Q_A^-/Q_A)$ values of *T. elongatus* and spinach were estimated to be −140 and −162 mV, respectively, by fluorescence spectroelectrochemical measurements using identical redox mediators. It is speculated that a higher $E_m(Q_A^-/Q_A)$, hence a larger E_m gap between $Pheo_{D1}$ and Q_A, could be necessary to optimize the charge recombination rate at a high temperature in the thermophilic cyanobacterium *T. elongatus*.

The above observation of the similar $E_m(Q_A^-/Q_A)$ values between the intact and Mn-depleted PSII preparations is in sharp contrast to the previous results of redox titration using fluorescence measurement, in which the upshift of $E_m(Q_A^-/Q_A)$ by more than 100 mV has been observed upon Mn or Ca depletion [21–29]. To understand the reason for this discrepancy between the FTIR and fluorescence measurements, we performed fluorescence spectroelectrochemical measurements using the same PSII core complexes, OTTLE cell, and redox mediators as used in the above FTIR measurements (Fig. 3). The Nernst plots of the fluorescence intensities showed the E_m values of −110 ± 5 and +6 ± 3 mV for the intact and Mn-depleted PSII samples, respectively, providing an upshift of 116 mV by Mn depletion, which is consistent with the previous fluorescence results [21–29] (Fig. 3d and Table 1). The intact PSII showed an E_m value (−110 mV) similar to that estimated by FTIR measurement (−128 mV), but the former was slightly higher than the latter. This difference could be partly due to the effect of freeze and thaw, which was previously reported to provide a higher E_m value in fluorescence measurement [28]. It was further shown that when measuring light (430 nm) for fluorescence is attenuated by a factor of 10 (Fig. 3c), the E_m value of the Mn-depleted PSII downshifted to −32 ± 6 mV (Fig. 3d, green line), which provided a smaller gap of 78 mV from the intact sample. In these fluorescence measurements, solutions of the PSII core complexes were used, whereas pellet preparations in the presence of polyethylene glycol (PEG) were used for FTIR measurements. However, even when the same pellet preparations were used for fluorescence measurements, similar $E_m(Q_A^-/Q_A)$ values, −104 ± 5 and +8 ± 5 mV for the intact and Mn-depleted PSII core complexes, respectively, were obtained (Fig. S6), confirming that the forms of preparations (solution or pellet) do not affect the results.

4. Discussion

It has long been shown by redox titration using fluorescence detection that $E_m(Q_A^-/Q_A)$ upshifts by 100–160 mV upon depletion of the Mn_4CaO_5 cluster or more specifically Ca^{2+} removal from the cluster [21–29]. However, the present FTIR spectroelectrochemical measurements, which directly detect the redox state of Q_A without any interference with the photoreactions in PSII by infrared light, showed that in both the preparations of the PSII membranes from spinach and the PSII core complexes from *T. elongatus*, the $E_m(Q_A^-/Q_A)$ values were virtually unchanged by depletion of the Mn_4CaO_5 cluster (Fig. 2, Table 1). These results are highly reliable because the same effect of Mn depletion was observed for different preparations (PSII membranes vs. isolated PSII core complexes) from different species (a higher plant, spinach vs. a cyanobacterium, *T. elongatus*) under different measurement conditions (continuous illumination with DCMU vs. a single flash in the absence of herbicide). It is thus concluded that the presence or absence of the Mn_4CaO_5 cluster does not affect the E_m of Q_A on the electron acceptor side of PSII.

This conclusion is consistent with various previous observations on the properties of Q_A and relevant redox cofactors on the electron acceptor side: (i) the Q_A^-/Q_A FTIR difference spectrum was virtually unchanged upon Mn depletion, indicative of no changes in the interactions of Q_A and its immediate surroundings [35], (ii) there was no change in the redox equilibrium between Q_A^- and Q_B^- by Mn depletion in thylakoids [15], (iii) the electron transfer rate from Q_A^- to Q_B did not change by Ca^{2+} depletion [36], (iv) no change was observed in the trapping dynamics in PSII upon Mn depletion [56], (v) a thermoluminescence band due to $Q_A^-Y_D\cdot$ recombination around 45–50 °C did not differ significantly between intact and Ca^{2+}-depleted PSII samples [57], (vi) no large change by Mn depletion was observed in the E_m's of Q_B and the non-heme iron [33,34], which are strongly coupled with Q_A through His side chains, and (vii) any structural rearrangement was not observed on the electron acceptor side upon removal of the Mn_4CaO_5 cluster from PSII crystals in the X-ray diffraction study [58].

There was, however, a report that showed a result inconsistent with our conclusion. Andréasson et al. [37] observed the diminish of the ~400 μs decay transient of fluorescence upon Ca^{2+} removal by NaCl/EGTA wash in spinach PSII membranes, although there was no effect on this phase by NaCl wash, which removed the PsbP and PsbQ proteins. They thus concluded that Ca^{2+} depletion inhibits the Q_A^- to Q_B electron transfer. However, this conclusion is opposite to that of the recent report by Semin et al. [36] (above observation (iii)), who did not detect such an effect of Ca^{2+} depletion on the Q_A^- to Q_B kinetics using similar fluorescence detection. They further showed that the removal of the PsbP and PsbQ proteins by NaCl wash retarded the Q_A^- to Q_B electron transfer, which was consistent with the previous observation by Roose et al. [59]. These results of the effect of the PsbP and PsbQ proteins were however inconsistent with the observation by Andréasson et al. [37]. Thus, there are discrepancies even in the previous reports about the effect of Ca^{2+} and the extrinsic proteins on the Q_A^- to Q_B electron transfer. Our SDS-PAGE analysis of the Mn-depleted samples after NH_2OH treatment showed that PsbP and PsbQ were partially removed from the spinach PSII membranes, whereas PsbV, PsbU, and PsbO were mostly removed from the PSII core complexes from *T. elongatus* (Fig.

S7). Thus, although it seems that binding of the extrinsic proteins does not affect the $E_m(Q_A^-/Q_A)$ at least in the PSII core complexes of *T. elongatus*, we could not draw any conclusion about the effect of the extrinsic proteins on $E_m(Q_A^-/Q_A)$ in spinach PSII membranes. Further studies are necessary to reach a final conclusion about the effect of the extrinsic proteins on $E_m(Q_A^-/Q_A)$. Also, the effect of Mn/Ca depletion on the kinetics of electron transfer from Q_A to Q_B needs to be examined to confirm the conclusion in the present study.

The significant question is why the result of the FTIR measurement on the Mn-depletion effect on $E_m(Q_A^-/Q_A)$ is so different from the previous results by fluorescence measurement [21–29]. Estimation of $E_m(Q_A^-/Q_A)$ by fluorescence spectroelectrochemistry using the same PSII core preparation, OTTLE cell, and redox mediators as used in the FTIR measurements showed a significantly high value in the Mn-depleted PSII (+6 − +8 mV in comparison with −138 mV by FTIR) resulting in a large $E_m(Q_A^-/Q_A)$ gap of 110–120 mV from intact PSII (Figs. 3 and S3, Table 1), as has been shown in the previous fluorescence studies [21–29]. Thus, the discrepancy between the FTIR and fluorescence results purely originates from the difference in these detection methods. In contrast to the FTIR spectroscopy, fluorescence measurement rather indirectly monitors the redox state of Q_A. It is known that a fluorescence intensity does not necessarily show a linear relationship with a Q_A^- population [60,61]. However, the non-linear relationship may not be the direct reason for the significant difference in the estimated $E_m(Q_A^-/Q_A)$ values between the intact and Mn-depleted PSII, because linearity correction shifts both the E_m values in the positive direction. In the case of the present results, the $E_m(Q_A^-/Q_A)$ values, which were corrected using F_m/F_0 values [24], are −94 and +18 mV for the intact and Mn-depleted PSII core complexes (from uncorrected values of −110 and +6 mV, respectively), still providing a ~110 mV difference. When excitation light (430 nm) attenuated by a factor of 10 (0.001 μE s^{-1} m^{-2}) was used for fluorescence measurement of the Mn-depleted PSII, the $E_m(Q_A^-/Q_A)$ value was estimated to be lower by 38 mV, providing a smaller $E_m(Q_A^-/Q_A)$ gap (78 mV) from the intact PSII (Fig. 3d). The problem thus could be perturbation of the redox state of Q_A by weak visible light for excitation of PSII to monitor fluorescence.

The excitation rate by light absorption, k_{abs}, is estimated from a photon flux (F) and an absorption cross section (σ) by an equation, $k_{abs} = \sigma F$. The absorption cross section σ (cm^2) is related to an extinction coefficient ε (M^{-1} cm^{-1}) as $\sigma = 10^3 \cdot \ln 10 \cdot \varepsilon / N_A$, where N_A is the Avogadro constant. From ε_{431nm} = 96.0 mM^{-1} cm^{-1} for Chl*a* [62], σ is estimated to be 3.67×10^{-16} cm^2 at ~430 nm. Because the monomeric PSII core complex has 35 Chls per a reaction center [10], the rate of Q_A^- formation by light-induced charge separation, $k(Q_A^-)$, is expressed as $k(Q_A^-) = 35 \times k_{abs}$, and its time constant, $\tau(Q_A^-)$, is obtained by $\tau(Q_A^-) = 1/k(Q_A^-)$. When F at 430 nm is 0.001 μE s^{-1} m^{-2}, which is used in our fluorescence measurement as a very weak excitation light (Fig. 3), $\tau(Q_A^-)$ is estimated to be 21.6 min. The relaxation of photoinduced Q_A^- in Mn-depleted PSII is very slow and takes hours at relatively low potentials (which is the main reason why we relaxed Q_A^- at a high potential of +350 mV for 60 min after every measurements), because an electron hole must be transferred to peripheral electron donors such as cytochrome b_{559} or to mediators. Thus, Q_A^- tends to accumulate in Mn-depleted PSII even under very weak light such as 0.001 μE s^{-1} m^{-2} at lower electrode potentials. This would be the reason why the $E_m(Q_A^-/Q_A)$ estimated by fluorescence showed a higher value with stronger measuring light. In contrast to fluorescence measurement, the FTIR method uses infrared light as measuring light that does not interfere with the redox reactions of cofactors in PSII, and hence it can properly monitor the redox state of Q_A.

It was previously shown that $E_m(Q_A^-/Q_A)$ is altered depending on the species of herbicide bound at the Q_B site [23]; PSII with DCMU showed an $E_m(Q_A^-/Q_A)$ value higher by ~100 mV than that with phenolic herbicide such as bromoxynil and ioxynil. This herbicide dependence of $E_m(Q_A^-/Q_A)$ was reflected by a higher peak temperature of thermoluminescence due to $S_2Q_A^-$ recombination in the presence of DCMU than in the presence of phenolic herbicide [23,50]. Moreover, the difference in the hydrogen bond interactions at the CO groups of Q_A^- depending on the herbicide species was detected by FTIR difference spectroscopy [50], and the propagation of the herbicide interaction at the Q_B site to Q_A to affect the $E_m(Q_A^-/Q_A)$ was demonstrated by theoretical calculations [63]. Such a herbicide-induced $E_m(Q_A^-/Q_A)$ change suggests the possible presence of an $E_m(Q_A^-/Q_A)$ regulation mechanism by the status of the Q_B site, i.e., neutral plastoquinone (PQ), a singly reduced PQ anion, and an empty Q_B pocket. Furthermore, it was recently reported that $E_m(Q_A^-/Q_A)$ upshifts upon removal of bicarbonate from the non-heme iron. Indeed, the time constant of electron transfer from Q_A^- to Q_B was slowed by bicarbonate depletion [29]. These $E_m(Q_A^-/Q_A)$ shifts are reasonable when considering the close interaction of Q_A with the non-heme iron and Q_B through the Q_A-His-Fe-His-Q_B bridge.

Thus, from the present observation of the absence of the $E_m(Q_A^-/Q_A)$ shift upon Mn depletion, together with the previous results of little effect of Mn depletion on $E_m(Q_B^-/Q_B)$ and $E_m(Fe^{2+}/Fe^{3+})$ [33,34], it is concluded that the Mn_4CaO_5 cluster on the electron donor side does not directly regulate the E_m levels of the quinone and iron cofactors on the electron acceptor side. This is consistent with the fact that the Mn_4CaO_5 cluster and the quinone-iron complex are separated by more than 40 Å across the membrane spanning helices. Rather, the redox reactions of the quinone electron acceptors are regulated by changes in the immediate environment such as changes in pH and a bicarbonate level in the stroma [16,29], while the electron donor side communicates with the electron acceptor side mainly via a cyclic electron transfer consisting of β-carotene, Chl_Z, and cytochrome b_{559} [64,65]. It is still an open question, however, whether structural changes on the electron donor side by interactions of the extrinsic proteins regulate the electron transfer reactions of the quinone electron acceptors in PSII [36,37,59].

5. Conclusion

FTIR spectroelectrochemical measurement, which can directly monitor the redox state of Q_A at different electrode potentials, showed that $E_m(Q_A^-/Q_A)$ in PSII was virtually unchanged upon depletion of the Mn_4CaO_5 cluster (Fig. 2). This is in sharp contrast to the previous results by fluorescence measurement that $E_m(Q_A^-/Q_A)$ upshifts by more than 100 mV when the Mn_4CaO_5 cluster is inactivated [21–29]. This discrepancy possibly arises from weak visible light for fluorescence excitation that could perturb the Q_A redox state especially in Mn-depleted PSII, which was supported by fluorescence spectroelectrochemical measurement using excitation light at different intensities (Fig. 3). Using infrared light for monitoring Q_A, FTIR spectroelectrochemistry is free from such perturbation and hence can estimate an accurate $E_m(Q_A^-/Q_A)$ value. From the absence of the effect of Mn depletion on $E_m(Q_A^-/Q_A)$ as well as little effect on $E_m(Q_B^-/Q_B)$ and $E_m(Fe^{2+}/Fe^{3+})$ [33,34], it is concluded that the Mn_4CaO_5 cluster does not directly regulate the redox potentials of the iron-quinone electron acceptors on the electron acceptor side of PSII, although the effect of the extrinsic proteins is still a question to be answered.

Abbreviations

DCMU	3-(3,4-dichlorophenyl)-1,1-dimethylurea
FTIR	Fourier transform infrared
E_m	redox potential
methoxy-PMS	1-methoxy-5-methylphanazinium methosulfate
OTTLE	optically transparent thin-layer electrode
PEG	polyethylene glycol
SHE	standard hydrogen electrode
TMPD	*N*,*N*,*N*′,*N*′-tetramethyl-*p*-phenylenediamine

Transparency document

The Transparency document associated with this article can be found, in online version.

Acknowledgements

This study was supported by JSPS KAKENHI (JP16K17854, JP17H05721 to Y.K., JP17H06433, JP17H06435, JP17H03662 to T.N., JP17K07442 to R.N.).

Appendix A. Supplementary data

Supplementary data to this article can be found online at https://doi.org/10.1016/j.bbabio.2019.148082.

References

[1] J. Barber, Photosynthetic energy conversion: natural and artificial, Chem. Soc. Rev. 38 (2009) 185–196.
[2] I. McConnell, G.H. Li, G.W. Brudvig, Energy conversion in natural and artificial photosynthesis, Chem. Biol. 17 (2010) 434–447.
[3] D.J. Vinyard, G.M. Ananyev, G.C. Dismukes, Photosystem II: the reaction center of oxygenic photosynthesis, Annu. Rev. Biochem. 82 (2013) 577–606.
[4] J.-R. Shen, The structure of photosystem II and the mechanism of water oxidation in photosynthesis, Annu. Rev. Plant Biol. 66 (2015) 23–48.
[5] F. Rappaport, B.A. Diner, Primary photochemistry and energetics leading to the oxidation of the $(Mn)_4Ca$ cluster and to the evolution of molecular oxygen in photosystem II, Coord. Chem. Rev. 252 (2008) 259–272.
[6] H. Dau, I. Zaharieva, Principles, efficiency, and blueprint character of solar-energy conversion in photosynthetic water oxidation, Acc. Chem. Res. 42 (2009) 1861–1870.
[7] T. Cardona, A. Sedoud, N. Cox, A.W. Rutherford, Charge separation in photosystem II: a comparative and evolutionary overview, Biochim. Biophys. Acta, Bioenerg. 1817 (2012) 26–43.
[8] P. Joliot, G. Barbieri, R. Chabaud, Model of the System II photochemical centers, Photochem. Photobiol. 10 (1969) 309–329.
[9] B. Kok, B. Forbush, M. McGloin, Cooperation of charges in photosynthetic O_2 evolution-I. A linear four step mechanism, Photochem. Photobiol. 11 (1970) 457–475.
[10] Y. Umena, K. Kawakami, J.-R. Shen, N. Kamiya, Crystal structure of oxygen-evolving photosystem II at a resolution of 1.9 Å, Nature 473 (2011) 55–60.
[11] V. Petrouleas, A.R. Crofts, The quinone iron acceptor complex, in: T. Wydrzynski, K. Satoh (Eds.), Photosystem II: The Light-Driven Water:Plastoquinone Oxidoreductase, Springer, Dordrecht, 2005, pp. 177–206.
[12] F. Müh, C. Glöckner, J. Hellomich, A. Zouni, Light-induced quinone reduction in photosystem II, Biochim. Biophys. Acta, Bioenerg. 1817 (2012) 44–65.
[13] P.B. Kos, Z. Deak, O. Cheregi, I. Vass, Differential regulation of *psbA* and *psbD* gene expression, and the role of the different D1 protein copies in the cyanobacterium *Thermosynechococcus elongatus* BP-1, Biochim. Biophys. Acta, Bioenerg. 1777 (2008) 74–83.
[14] A.K. Clarke, A. Soitamo, P. Gustafsson, G. Oquist, Rapid interchange between two distinct forms of cyanobacterial photosystem II reaction-center protein D1 in response to photoinhibition, Proc. Natl. Acad. Sci. U. S. A. 90 (1993) 9973–9977.
[15] H.H. Robinson, A.R. Crofts, Kinetics of proton uptake and the oxidation-reduction reactions of the quinone acceptor complex of PS II from pea chloroplasts, in: C. Sybesma (Ed.), Advances in Photosynthesis Research, Springer, Dordrecht, 1984, pp. 477–480.
[16] Y. Nozawa, T. Noguchi, pH-Dependent regulation of the relaxation rate of the radical anion of the secondary quinone electron acceptor Q_B in photosystem II as revealed by Fourier transform infrared spectroscopy, Biochemistry 57 (2018) 2828–2836.
[17] D. Lazár, Chlorophyll *a* fluorescence induction, Biochim. Biophys. Acta, Bioenerg. 1412 (1999) 1–28.
[18] G.C. Papageorgiou, Govindjee, Photosystem II fluorescence: slow changes – scaling from the past, J. Photochem. Photobiol. B Biol. 104 (2011) 258–270.
[19] G. Schansker, S.Z. Toth, A.R. Holzwarth, G. Garab, Chlorophyll *a* fluorescence: beyond the limits of the Q_A model, Photosynth. Res. 120 (2014) 43–58.
[20] H.M. Kalaji, G. Schansker, R.J. Ladle, V. Goltsev, K. Bosa, S.I. Allakhverdiev, M. Brestic, F. Bussotti, A. Calatayud, P. Dąbrowski, N.I. Elsheery, L. Ferroni, L. Guidi, S.W. Hogewoning, A. Jajoo, A.N. Misra, S.G. Nebauer, S. Pancaldi, C. Penella, D.B. Poli, M. Pollastrini, Z.B. Romanowska-Duda, B. Rutkowska, J. Serôdio, K. Suresh, W. Szulc, E. Tambussi, M. Yanniccari, M. Zivcak, Frequently asked questions about in vivo chlorophyll fluorescence: practical issues, Photosynth. Res. 122 (2014) 121–158.
[21] A. Krieger, A.W. Rutherford, G.N. Johnson, On the determination of redox midpoint potential of the primary quinone electron acceptor, Q_A, in photosystem II, Biochim. Biophys. Acta, Bioenerg. 1229 (1995) 193–201.
[22] G.N. Johnson, A.W. Rutherford, A. Krieger, A change in the midpoint potential of the quinone Q_A in photosystem II associated with photoactivation of oxygen evolution, Biochim. Biophys. Acta, Bioenerg. 1229 (1995) 202–207.
[23] A. Krieger-Liszkay, A.W. Rutherford, Influence of herbicide binding on the redox potential of the quinone acceptor in photosystem II: relevance to photodamage and phytotoxicity, Biochemistry 37 (1998) 17339–17344.
[24] T. Shibamoto, Y. Kato, M. Sugiura, T. Watanabe, Redox potential of the primary plastoquinone electron acceptor Q_A in photosystem II from *Thermosynechococcus elongatus* determined by spectroelectrochemistry, Biochemistry 48 (2009) 10682–10684.
[25] T. Shibamoto, Y. Kato, R. Nagao, T. Yamazaki, T. Tomo, T. Watanabe, Species-dependence of the redox potential of the primary quinone electron acceptor Q_A in photosystem II verified by spectroelectrochemistry, FEBS Lett. 584 (2010) 1526–1530.
[26] K. Ido, C.M. Gross, F. Guerrero, A. Sedoud, T.-L. Lai, K. Ifuku, A.W. Rutherford, A. Krieger-Liszkay, High and low potential forms of the Q_A quinone electron acceptor in photosystem II of *Thermosynechococcus elongatus* and spinach, J. Photochem. Photobiol. B 104 (2011) 154–157.
[27] S.I. Allakhverdievm, T. Tsuchiya, K. Watabe, A. Kojima, D.A. Los, T. Tomo, V.V. Klimov, M. Mimuro, Redox potentials of primary electron acceptor quinone molecule $(Q_A)^-$ and conserved energetics of photosystem II in cyanobacteria with chlorophyll *a* and chlorophyll *d*, Proc. Natl. Acad. Sci. U. S. A. 108 (2011) 8054–8058.
[28] Y. Kato, T. Shibamoto, S. Yamamoto, T. Watanabe, N. Ishida, M. Sugiura, F. Rappaport, A. Boussac, Influence of the PsbA1/PsbA3, Ca^{2+}/Sr^{2+} and Cl^-/Br^- exchanges on the redox potential of the primary quinone Q_A in Photosystem II from *Thermosynechococcus elongatus* as revealed by spectroelectrochemistry, Biochim. Biophys. Acta, Bioenerg. 1817 (2012) 1998–2004.
[29] K. Brinkert, S.D. Causmaecker, A. Krieger-Liszkay, A. Fantuzzi, A.W. Rutherford, Bicarbonate-induced redox tuning in photosystem II for regulation and protection, Proc. Natl. Acad. Sci. U. S. A. 113 (2016) 12144–12149.
[30] A. Krieger-Liszkay, C. Fufezan, A. Trebst, Singlet oxygen production in photosystem II and related protection mechanism, Photosynth. Res. 98 (2008) 551–564.
[31] A.W. Rutherford, A. Osyczka, F. Rappaport, Back-reactions, short-circuits, leaks and other energy wasteful reactions in biological electron transfer: redox tuning to survive life in O_2, FEBS Lett. 586 (2012) 603–616.
[32] I. Vass, Role of charge recombination processes in photodamage and photoprotection of the photosystem II complex, Physiol. Plant. 142 (2011) 6–16.
[33] Y. Kato, R. Nagao, T. Noguchi, Redox potential of the terminal quinone electron acceptor Q_B in photosystem II revealing the mechanism of electron-transfer regulation, Proc. Natl. Acad. Sci. U. S. A. 113 (2016) 620–625.
[34] Y. Kato, T. Noguchi, Long-range interaction between the Mn_4CaO_5 cluster and the non-heme iron center in photosystem II as revealed by FTIR spectroelectrochemistry, Biochemistry 53 (2014) 4914–4923.
[35] Y. Kato, R. Ishii, T. Noguchi, Comparative analysis of the interaction of the primary quinone Q_A in intact and Mn-depleted photosystem II membranes using light-induced ATR-FTIR spectroscopy, Biochemistry 55 (2016) 6355–6358.
[36] B.K. Semin, L.N. Davletshina, M.D. Mamedov, Effect of different methods of Ca^{2+} extraction from PSII oxygen-evolving complex on the Q_A^- oxidation kinetics, Photosynth. Res. 136 (2018) 83–91.
[37] L.-E. Andréasson, I. Vass, S. Styring, Ca^{2+} depletion modifies the electron transfer on both donor and acceptor sides in photosystem II from spinach, Biochim. Biophys. Acta, Bioenerg. 1230 (1995) 155–164.
[38] Y. Kato, T. Noguchi, FTIR spectroelectrochemistry combined with a light-induced difference technique: application to the iron-quinone electron acceptor in photosystem II, Biomed. Spectrosc. Imaging 5 (2016) 269–282.
[39] T. Noguchi, C. Berthomieu, Molecular analysis by vibrational spectroscopy, in: T. Wydrzynski, K. Satoh (Eds.), Photosystem II: The Light-Driven Water:Plastoquinone Oxidoreductase, Springer, Dordrecht, 2005, pp. 367–387.
[40] H.-A. Chu, Fourier transform infrared difference spectroscopy for studying the molecular mechanism of photosynthetic water oxidation, Front. Plant Sci. 4 (2013) 146.
[41] R.J. Debus, FTIR studies of metal ligands, networks of hydrogen bonds, and water molecules near the active site Mn_4CaO_5 cluster in photosystem II, Biochim. Biophys. Acta, Bioenerg. 1847 (2015) 19–34.
[42] T. Noguchi, Fourier transform infrared difference and time-resolved infrared detection of the electron and proton transfer dynamics in photosynthetic water oxidation, Biochim. Biophys. Acta, Bioenerg. 1847 (2015) 35–45.
[43] F. Rappaport, M. Guergova-Kuras, P.J. Nixon, B.A. Diner, J. Lavergne, Kinetics and pathways of charge recombination in photosystem II, Biochemistry 41 (2002) 8518–8527.
[44] M. Grabolle, H. Dau, Energetics of primary and secondary electron transfer in photosystem II membrane particles of spinach revisited on basis of recombination-fluorescence measurements, Biochim. Biophys. Acta Bioenerg. 1708 (2005) 209–218.
[45] D.A. Berthold, G.T. Babcock, C.F. Yocum, A highly resolved, oxygen-evolving photosystem II preparation from spinach thylakoid membranes – EPR and electron-transport properties, FEBS Lett. 134 (1981) 231–234.
[46] T. Ono, Y. Inoue, Effects of removal and reconstitution of the extrinsic 33, 24 and 16 kDa proteins on flash oxygen yield in photosystem II particles, Biochim. Biophys. Acta, Bioenerg. 850 (1986) 380–389.
[47] M. Iwai, T. Suzuki, A. Kamiyama, I. Sakurai, N. Dohmae, Y. Inoue, M. Ikeuchi, The PsbK subunit is required for the stable assembly and stability of other small subunits in the PSII Complex in the thermophilic cyanobacterium *Thermosynechococcus elongatus* BP-1, Plant Cell Physiol. 51 (2010) 554–560.
[48] S. Nakamura, R. Nagao, R. Takahashi, T. Noguchi, Fourier transform infrared detection of a polarizable proton trapped between photooxidized tyrosine Y_Z and a coupled histidine in photosystem II. Relevance to the proton transfer mechanism of

water oxidation, Biochemistry 53 (2014) 3131–3144.
[49] R. Nagao, T. Tomo, T. Noguchi, Effects of extrinsic proteins on the protein conformation of the oxygen-evolving center in cyanobacterial photosystem II as revealed by Fourier transform infrared spectroscopy, Biochemistry 54 (2015) 2022–2031.
[50] C. Berthomieu, E. Nabedryk, W. Mäntele, J. Breton, Characterization by FTIR spectroscopy of the photoreduction of the primary quinone acceptor Q_A in photosystem II, FEBS Lett. 269 (1990) 363–367.
[51] H. Suzuki, M. Nagasaka, M. Sugiura, T. Noguchi, Fourier transform infrared spectrum of the secondary quinone electron acceptor Q_B in photosystem II, Biochemistry 44 (2005) 11323–11328.
[52] A. Takano, R. Takahashi, H. Suzuki, T. Noguchi, Herbicide effect on the hydrogen-bonding interaction of the primary quinone electron acceptor Q_A in photosystem II as studied by Fourier transform infrared spectroscopy, Photosynth. Res. 98 (2008) 159–167.
[53] T. Noguchi, T. Ono, Y. Inoue, Direct detection of a carboxylate bridge between Mn and Ca^{2+} in the photosynthetic oxygen-evolving center by means of Fourier transform infrared spectroscopy, Biochim. Biophys. Acta, Bioenerg. 1228 (1995) 189–200.
[54] T. Noguchi, M. Sugiura, Analysis of flash-induced FTIR difference spectra of the S-state cycle in the photosynthetic water-oxidizing complex by uniform ^{15}N and ^{13}C isotope labeling, Biochemistry 42 (2003) 6035–6042.
[55] S. Nakamura, T. Noguchi, Quantum mechanics/molecular mechanics simulation of the ligand vibrations of the water-oxidizing Mn_4CaO_5 cluster in photosystem II, Proc. Natl. Acad. Sci. U. S. A. 113 (2016) 12727–12732.
[56] L.M.C. Barter, M.J. Schilstra, J. Barber, J.R. Durrant, D.R. Klug, Are the trapping dynamics in photosystem II sensitive to Q_A redox potential? J. Photochem. Photobiol. A 142 (2001) 127–132.
[57] G.N. Johnson, A. Boussac, A.W. Rutherford, The origin of 40–50 °C thermoluminescence bands in photosystem II, Biochim. Biophys. Acta, Bioenerg. 1184 (1994) 85–92.
[58] M. Zhang, M. Bommer, R. Chatterjee, R. Hussein, J. Yano, H. Dau, J. Kern, H. Dobbek, A. Zouni, Structural insights into the light-driven auto-assembly process of the water-oxidizing Mn_4CaO_5-cluster in photosystem II, eLife 6 (2017) e26933.
[59] J.L. Roose, L.K. Frankel, T.M. Bricker, Documentation of significant electron transport defects on the reducing side of photosystem II upon removal of the PsbP and PsbQ extrinsic proteins, Biochemistry 49 (2010) 36–41.
[60] G. Paillotin, Movement of excitations in photosynthetic domains of photosystem II, J. Theor. Biol. 58 (1976) 237–252.
[61] J. Lavergne, H.W. Trissl, Theory of fluorescence induction in photosystem II: derivation of analytical expressions in a model including exciton-radical-pair equilibrium and restricted energy transfer between photosynthetic units, Biophys. J. 68 (1995) 2474–2492.
[62] C. Eijckelhoff, J.P. Dekker, A routine method to determine the chlorophyll *a*, pheophytin *a* and β-carotene contents of isolated photosystem II reaction center complexes, Photosynth. Res. 52 (1997) 69–73.
[63] H. Ishikita, K. Hasegawa, T. Noguchi, How does the Q_B site influence propagate to the Q_A site in photosystem II? Biochemistry 50 (2011) 5436–5442.
[64] C.A. Tracewell, A. Cua, D.H. Stewart, D.F. Bocian, G.W. Brudvig, Characterization of carotenoid and chlorophyll photooxidation in photosystem II, Biochemistry 40 (2001) 193–203.
[65] K.E. Shinopoulos, G.W. Brudvig, Cytochrome b_{559} and cyclic electron transfer within photosystem II, Biochim. Biophys. Acta, Bioenerg. 1817 (2012) 66–75.